Journal of Experimental Nanoscience

Publication details, including instructions for authors and subscription information:
http://www.informaworld.com/smpp/title~content=t716100757

An in situ STM study of cobalt electrodeposition on Au(111) in $BMIBF_4$ ionic liquid

Long-Gang Lin[a]; Jia-Wei Yan[a]; Yu Wang[a]; Yong-Chun Fu[a]; Bing-Wei Mao[a]
[a] Chemistry Department and State Key Laboratory of Physical Chemistry of Solid Surfaces, College of Chemistry and Chemical Engineering, Xiamen University, Xiamen 361005, China

To cite this Article Lin, Long-Gang , Yan, Jia-Wei , Wang, Yu , Fu, Yong-Chun and Mao, Bing-Wei(2006) 'An **in situ** STM study of cobalt electrodeposition on Au(111) in $BMIBF_4$ ionic liquid', Journal of Experimental Nanoscience, 1: 3, 269 — 278

To link to this Article: DOI: 10.1080/17458080601009643

URL: http://dx.doi.org/10.1080/17458080601009643

Journal of Experimental Nanoscience,
Vol. 1, No. 3, September 2006, 269–278

Taylor & Francis
Taylor & Francis Group

An *in situ* STM study of cobalt electrodeposition on Au(111) in $BMIBF_4$ ionic liquid

LONG-GANG LIN, JIA-WEI YAN, YU WANG,
YONG-CHUN FU and BING-WEI MAO*

Chemistry Department and State Key Laboratory of Physical Chemistry
of Solid Surfaces, College of Chemistry and Chemical Engineering,
Xiamen University, Xiamen 361005, China

(*Received June 2006; in final form September 2006*)

The initial stage of Co electrodeposition on Au(111) from $CoCl_2$ and $Co(BF_4)_2$ in a room-temperature ionic liquid of $BMIBF_4$ is investigated by *in situ* STM. Preferential nucleation of Co at structure imperfections of the reconstructed Au(111) surface is observed for deposition from $CoCl_2$ at a surprisingly negative potential (−2.05 V vs. Pt wire). Monoatomic-height Co clusters of 2–3 nm in diameter are formed, which develop into Co islands with size confinement of 3–4 nm after prolonged deposition. The large driving force required for Co deposition from $CoCl_2$ is attributed to the molecular type of the salt in the ionic liquid together with the tip shielding effect. This is proved by the pronounced difference of Co deposition from $Co(BF_4)_2$, which takes place at a much less negative potential and proceeds in a 3D progressive nucleation and growth mode without preference in nucleation sites. Surface alloying accompanies the island formation, which is confirmed by pit generation upon stripping of the Co islands. The results are discussed in comparison with features of Co deposition in UHV and in aqueous solutions.

Keywords: Au(111); Cobalt; Electrodeposition; *In situ* STM; Room-temperature ionic liquids

1. Introduction

Preparation of ultrathin films of Co on noble metals such as Au(111) has received intensive attention since the magnetic properties of supported Co clusters such as perpendicular magnetization and the ferromagnetism to superparamagnetism transition show a close relationship to the nanostructures of the films [1, 2]. Although much of the work on Co deposition is carried out in UHV [3–8], electrodeposition has proven to be an important alternative in thin film preparation and efforts have also been devoted to Co electrodeposition on Au(111) in aqueous solutions [9–14]. On the other hand, structural characterization of the Co thin films has benefited from scanning tunneling microscopy (STM) in both UHV and aqueous solution environments, which provides

*Corresponding author. Email: bwmao@xmu.edu.cn

Journal of Experimental Nanoscience
ISSN 1745–8080 print/ISSN 1745–8099 online
http://www.tandf.co.uk/journals
DOI: 10.1080/17458080601009643

a close correlation between the structure and properties of the thin film. *In situ* STM results from aqueous solutions [10, 11] have shown pronounced difference with that from UHV [3, 4, 7] in the initial stage of Co deposition. Further comparative studies on Co deposition in solutions and in UHV are, therefore, of fundamental significance.

However, *in situ* STM studies on Co deposition in aqueous solutions have suffered from the concurrently large current produced from the hydrogen evolution reaction, which severely interferes with *in situ* STM imaging and possibly also the deposition process. Only a few *in situ* STM studies on Co electrodepostion have been reported in aqueous solutions [10, 11]. In fact, hydrogen evolution is a common problem in aqueous solution for electrodeposition of metals whose Nernst potentials overlap with or are more negative than that of the hydrogen evolution reaction. Although the problem can be avoided by using organic solvents of large electrochemical window, the traditional molecular type of organic solvents is too volatile to carry out *in situ* STM characterization of the deposition process. Room-temperature ionic liquids (RTILs), especially non-chloroaluminated RTIL such as those composed of substituted imidazolium cations and PF_6^-, BF_4^-, $CF_3SO_3^-$, and $(CF_3SO_2)_2N^-$ anions, are a new type of organic solvent, which offers wide electrochemical windows, vanishingly low vapor pressure and high conductivity [15–18] and thus have become popular organic solvents for the electrodeposition of a variety of metals and semiconductors [18–27]. It is only possible to carry out STM characterization in this type of organic solvent at potentials as negative as is necessary for electrodeposition of metals and semiconductors.

Freyland, Endres, and their coworkers, have reported *in situ* STM studies on the electrodeposition of a number of systems including transition metals, light metals and even elemental semiconductors in ionic liquid [18–20]. Preliminary *in situ* STM studies on Co and Co–Al alloy electrodeposition on Au(111) from a chloroaluminated $AlCl_3$/BMICl ionic liquid have also been reported by Zell and Freyland [23], which showed features of monatomic-height islands for Co deposition. However, because of the lack of clear STM images, details of such as registration of the Co deposit with the substrate surface are unclear. Furthermore, the presence of aluminum chloride used in that work restricts the cathodic potential limit in order to avoid Al codeposition. Thus, the control of potential is rather critical when Co deposition is the only concern.

In this paper, we present an *in situ* STM study of the initial stage of Co electrodeposition on Au(111) in non-chloroaluminated 1-butyl-3-methylimidazolium tetrafluoroborates ($BMIBF_4$) ionic liquid from two salts of Co(II): $CoCl_2$ and $Co(BF_4)_2$. We found very different behaviours between the two systems: Deposition from $CoCl_2$ initiates at very negative potential at the structure imperfections of the Au(111) reconstruction with Co clusters of 2–3 nm, while deposition from $Co(BF_4)_2$ takes place at a much less negative potential without preference in nucleation sites. Discussions are made in comparison with the features of Co deposition in UHV and in aqueous solutions.

2. Experimental

Synthesis of $BMIBF_4$ has been described in a previous paper [28]. Briefly, 1-butyl-3-methylimidazolium halide (BMICl) was first prepared followed by metathesis with

10% molar excess amount of aqueous HBF_4 solution. The solution was heated at 130°C to remove the excess HBF_4, H_2O and the by-product HCl via volatilization. The colorless or pale yellow liquid was then extracted into dichloromethane, and the organic phase was repeatedly washed with small volumes of water until no precipitation of AgCl occurred in the aqueous phase on addition of a concentrated $AgNO_3$ solution. The organic phase was then washed twice more with water to ensure complete removal of the residual chloride salt. The solvent water was removed *in vacuo* at 100°C for 12 h and the final liquid of $BMIBF_4$ is colorless or pale yellow.

Au single crystal beads were prepared and one of the facets of the Au beads was directly used for *in situ* STM measurements. For electrochemical measurements, the beads were orientated and polished to expose Au(111) surfaces large enough for hanging meniscus experiments. Prior to each experiment, the working surface was subjected to electrochemical polishing and flame annealing in an H_2 flame followed by cooling under N_2 protection. Electrochemical measurements were performed on a CHI electrochemical workstation (CH instrument, USA) in a conventional three-compartment cell. *In situ* STM measurements were carried out on a Nanoscope IIIa SPM (Digital Instrument, USA) under constant current. Electrochemically etched and thermosetting polyethylene insulated W tips were used for *in situ* STM measurements. Platinum wires were used as the quasi-reference electrodes for both electrochemical and *in situ* STM measurements. All chemicals used are AR grade. Solutions for Co deposition were prepared by dissolving $CoCl_2$ or $Co(BF_4)_2$ into the ionic liquid. No additional supporting electrolyte was added.

3. Results and discussions

The cyclic voltammogram of Au(111) from the ionic liquid containing $CoCl_2$ shows similar characteristic as in a pure ionic liquid, figure 1. The origin of the two small and broad cathodic peaks at −1.5 V (C_1) and −2.2 V (C_2) are unclear, but are likely related to the reduction of dissolved oxygen and a small amount of water molecules. No significant deposition and dissolution-related peaks of Co were observed, indicating that the Co deposition in this condition is very slow, if not impossible.

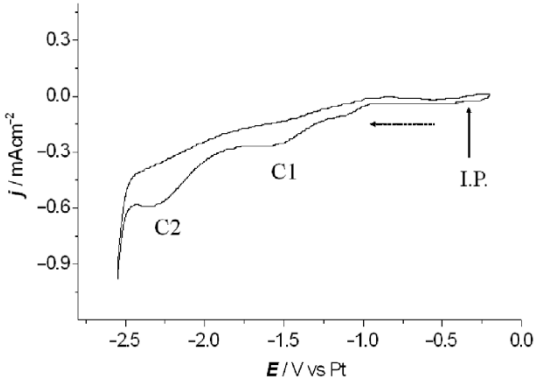

Figure 1. Cyclic voltammogram of Au(111) in $CoCl_2$ saturated $BMIBF_4$ solution. Scan rate: 100 mV/s.

In situ STM study in our previous work [28] has shown two significant effects from the $BMIBF_4$ ionic liquid: (1) long-range structural rearrangement of the Au surface upon cathodic potential excursion from −1.2 to −2.0 V; and (2) electrochemical annealing during the cathodic decomposition of the ionic liquid at −2.5 V. The structural rearrangement results in surface etching and thus places difficulties for *in situ* STM characterization of metal deposition such as Co on Au(111) that takes place in the noted potential windows. The problem could be alleviated by application of the following procedure: The ionic liquid is introduced at −0.5 V where an atomically flat surface is ensured. A potential step is applied to bring the surface directly to the annealing potential of −2.5 V to avoid structural rearrangement. This in turn builds up the well-known Au(111)($\sqrt{3} \times 23$) reconstruction. The potential is then moved anodically and slowly to a desired value of potential negative of −1.3 V (note that the structural rearrangement will set in again at potentials positive of −1.3 V). Additional ionic liquid containing the depositing metal ions is then introduced.

The potential for introducing $CoCl_2$ containing ionic liquid was −1.4 V, and the final concentration of $CoCl_2$ was 0.1 mM in the STM cell. The surface was monitored along with the gradual decrease of potential. Prior to Co deposition, the Au surface retained the feature of an electrochemically induced herringbone reconstruction. The periodicity (~6.45 nm) as well as the shape of the double rows show the usual Au(111) ($\sqrt{3} \times 22$) reconstruction, see figure 2(a). The double rows change in direction by 120° to relieve

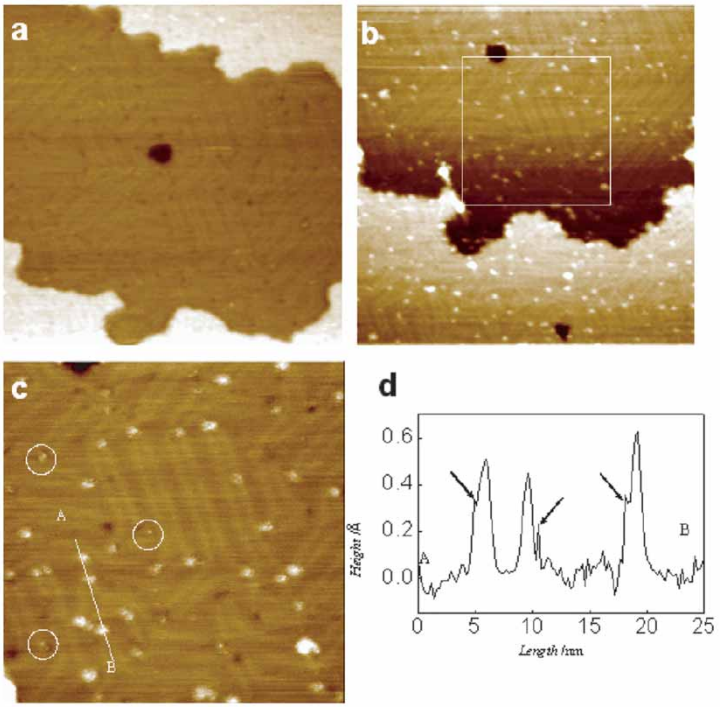

Figure 2. *In situ* STM characterization of Co electrodeposition on Au(111) in $BMIBF_4$ containing 0.1 mM $CoCl_2$ at −2.05 V: (a) Initiation of Co deposition; (b) 30 min. after (a); and (c) 40 min. after (a). (d) Cross-sectional analysis of (c). Scan size: 120 nm for (a) and (b), 60 nm for (c). $I_t = 1.8$ nA, $V_b = 0.1$ V tip positive.

the strain, but irregular changes in the direction of double rows also prevails in certain areas. These all introduce dislocation sites of the Au(111) reconstruction.

Co deposition from $CoCl_2$ took place at a surprisingly negative potential and at a very slow rate, which is not in conflict with the cyclic voltammogram. Tiny amounts of Co nuclei showed up at ~ -2.0 V, but a clear eye-catching amount of Co clusters was observed after further deposition of 20 min., figure 2(b). These clusters are nucleated preferentially at dislocation sites such as the elbow sites of the herringbone reconstruction. Step edge nucleation is also observed when the dislocation sites have been nearly taken up at a later stage. Close inspection of figure 2(c) and sectional analysis (figure 2d) reveals that the clusters are 2~3 nm in diameter and 0.6~0.9 Å in apparent height, much less than the height of the Co atomic layer. Interestingly, almost all clusters of this size are 'cloven' with small 'shoulders'. The rise of the 'shoulders' cannot be due to the artificial effect of the tip because the directions of the 'shoulders' are random with respect to the main bodies of the clusters. In addition, apart from these clusters, there are also smaller spots of 1 nm diameter (marked by circles) whose apparent height is as low as 0.47 Å. Reversal to a slightly positive potential leads to the dissolution of most of the clusters, but no pits were observed at the surface. This implies that deposition and dissolution processes are reversible at this very early stage and the structural imperfections act purely as the nucleation sites without involving surface alloying.

The size of the clusters is confined at 2~3 nm (figure 3a) during the electrodeposition of Co until after prolonged deposition or application of a gentle disturbance such as a slight decrease of potential or zooming into and out of a small part of the imaging area. Accomplished by further arrival of Co atoms to the Co clusters, there appears a transition from Co clusters to Co islands with marked increase in density and size of the clusters, figure 3(b). As shown in figure 3(c), islands of 6~7 nm in diameter and up to 3 Å in height are reached, which correspond to ~1000 atoms in each island. This size of the islands is large enough to form the bulk lattice of Co, although the shape of the Co islands is not well defined here. Islands at the step edges also prevail. At this island stage, surface alloying is involved (*infra vida*). Further growth of the islands was difficult even if the concentration of the $CoCl_2$ was increased or the potential was decreased considerably, except on regions some distance away from the imaging area where a relatively thicker film can be observed.

It can be seen from the above results that deposition of Co from $CoCl_2$ in a $BMIBF_4$ ionic liquid resembles the feature of molecular beam epitaxy deposition of Co in UHV, in which the point dislocations of the elbow site of the herringbone reconstruction act as the nucleation sites for Co deposition [3, 4, 7]. However, there exists a subtle difference between the two systems: Co deposition in UHV initiates with the formation of the bilayer-height and polygonal-shaped islands; whereas in the ionic liquid in the present work, there is a transformation from monatomic-height clusters at the very beginning to bilayer-height islands after a prolonged deposition. On the other hand, the dislocation-mediated nucleation behaviour in the ionic liquid is in contrast to the deposition mechanism in aqueous solutions [10, 11], the later following a layer-by-layer deposition mechanism with Moiré pattern in the STM images. Also in contrast is the very negative potential and abnormally slow rate of Co deposition in the ionic liquid than in the aqueous solutions. These phenomena are clear indications of significant media effects.

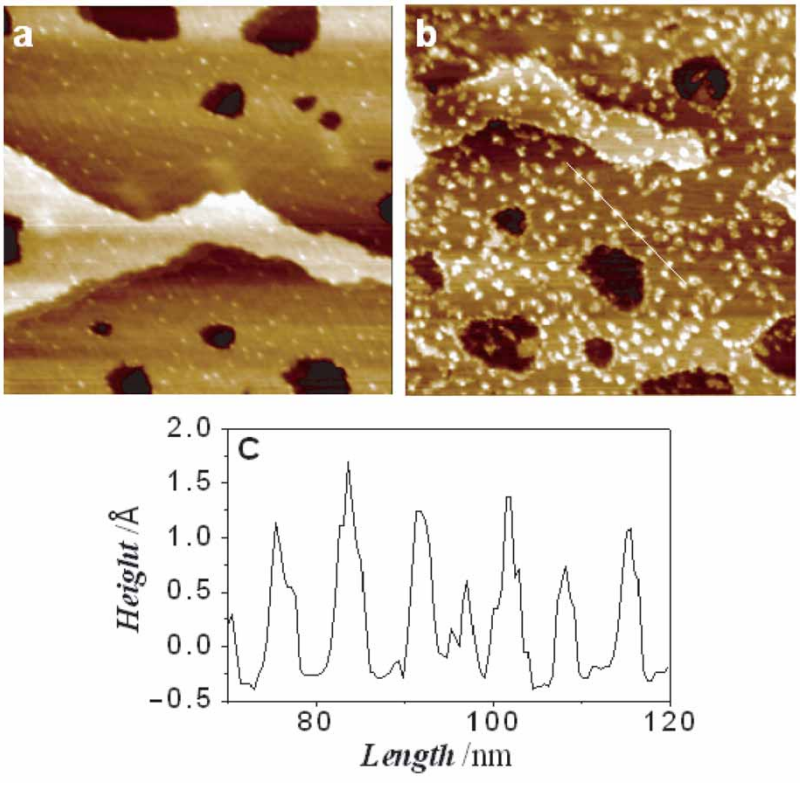

Figure 3. *In situ* STM observation of the growth of Co clusters on Au(111) at −2.01 V. (a) Smaller Co clusters after 15 min. deposition, and (b) larger Co clusters after 50 min. deposition. (c) Cross-sectional analysis of (b). Scan size: 125 nm × 125 nm for (a) and (b), $I_t = 2$ nA, $V_b = 0.4$ V tip positive. Solution as in figure 1.

According to our STM results, the potential (−2.05 V vs. Pt) to initiate Co deposition from $CoCl_2$ containing $BMIBF_4$ is equivalent to −1.65 V vs. SCE. This value is substantially more negative than the potential of Co at −0.75 (vs. SCE) for $CoSO_4$ [11] and −0.81 V for $CoCl_2$ [29] aqueous solutions. Direct comparison of this value with the previously reported work for Co electrodeposition in $AlCl_3$/BMICl ionic liquids is difficult since the latter were carried out using Co/Co^{2+} as reference electrode [24] without giving calibrations with respect to the SCE. Nevertheless, it is understood that $CoCl_2$ is a weak Lewis acid that could form a complex with an electron donation group depending on the environment. In aqueous solutions, the strongly polarized water molecules make Co(II) a solvated ion; while in ionic liquids, solvation may be a totally different situation. Since the BF_4^- anion is weakly coordinating, very likely $CoCl_2$ remains in a molecular type in $BMIBF_4$, which is expected to discharge at more negative potential than that of solvated Co(II) in aqueous solutions.

To verify the influence of the solution species of Co(II) on the thermodynamics of Co deposition, comparisons were made with deposition from $Co(BF_4)_2$ that has a common anion of BF_4^- as in $BMIBF_4$. Because BF_4^- is a weakly coordinating anion,

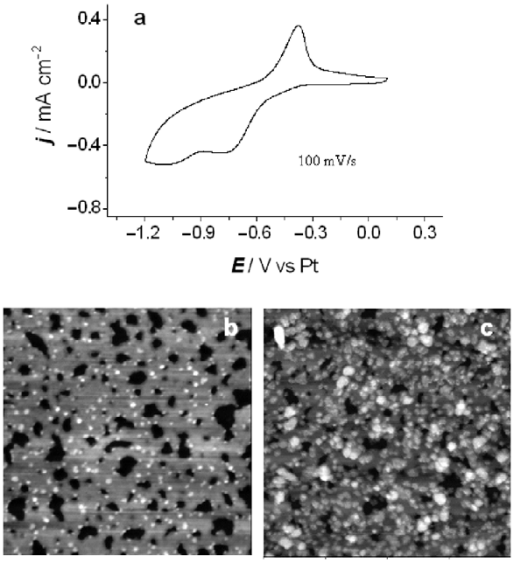

Figure 4. (a) Cyclic voltammogram of Au(111) in $BMIBF_4$ ionic liquid containing 1 mM $Co(BF_4)_2$. (b) and (c) STM images of Co electrodeposition on restructured Au(111) surface at −1.1 V. (c) was recorded 20 min. after (b). Scan size: 100 nm × 100 nm.

the $Co(BF_4)_2$ molecule is most likely dissociated to form 'naked' Co^{2+} in $BMIBF_4$. The experiments were carried out with other conditions fixed. From the cyclic voltammogram of Au(111) in 1 mM $BMIBF_4$, figure 4(a), a clear overpotential deposition peak can be identified at ~−0.7 V, which is typical of Co deposition from aqueous solutions. Unfortunately, the *in situ* STM characterization of Co deposition in this potential region is unfavourable because of the interference from the structural rearrangement of the surface as can be seen from figure 4(b). Nevertheless, in a fast experiment when etching of the surface is not yet too severe, monoatomic-height clusters of 1~2 nm are deposited at −1.1 V evenly at the surface without obvious site selection. This feature is similar to that reported by Zell and Freyland in a $AlCl_3$/BMICl ionic liquid [23]. We mention that because of the sever tip shielding in this system, the tip was withdrawn to initiate Co deposition and imaging of the surface was carried out 5 min. later. Once initiated, the clusters increase significantly in size and density with time, figure 4(b), revealing progressive nucleation and growth characteristics. It is thus clear that the precursors play a decisive role in the thermodynamics of Co deposition in the ionic liquid.

As for the slow kinetics of Co deposition from $CoCl_2$ in the ionic liquid, there are two possible reasons. Firstly, the viscosity of the $BMIBF_4$ is almost 180 times higher than that of water, which would hinder the diffusion of species. Indeed, it has been reported that diffusion coefficients of several species in pure $BMIBF_4$ (i.e. water free) are a few orders lower than the corresponding values in aqueous solutions [30]. It should be mentioned that absorbance of water from the atmosphere is inevitable even for hydrophobic $BMIBF_4$ during the *in situ* STM imaging in the present work. However,

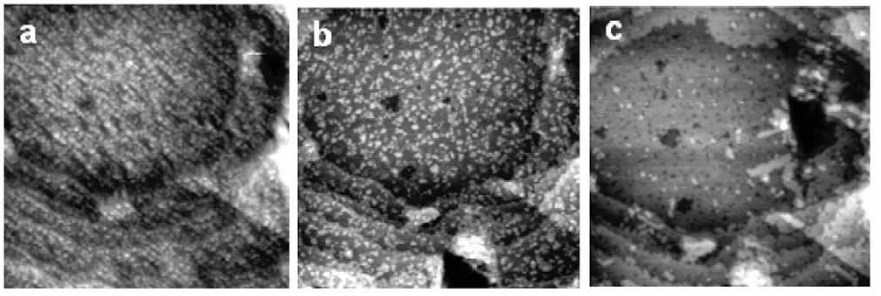

Figure 5. STM images of a granular Co deposit after 70 min. deposition at −2.05 V (a) and after partial (b) and complete (c) stripping of the Co deposit upon anodic potential excursion to −0.5 V (b) and −0.1 V (c). Images were recorded at an area not experienced with tip scanning during the deposition. The scattered islands left on the surface in (c) are Au islands formed due to site exchange with Co deposit. The large holes on the lower middle of (b) and upper right of (c) were produced unexpectedly by tip crashing due to fast dissolution of Co from the tip. Scan size 155 nm × 155 nm.

it has been found [30] that for neutral species the diffusion coefficient in $MDIBF_4$ (1-methyl-3-[2,6-(S)-dimethylocten-2-yl]imidazolium tetrafluoroborate) increases only slightly and reaches saturation with increase of water content. Therefore, the increase in diffusion coefficient of $CoCl_2$ due to lowering of the viscosity would be rather limited. Furthermore, in the ionic liquid $CoCl_2$ is likely near 'frozen' within the framework of the strong ionic atmosphere, leading to extremely slow mass transfer and thus slow rate of deposition. Secondly, tip shielding is also a factor that further slows down the deposition process as has been mentioned earlier. This is confirmed by scanning on a different area of the surface after prolonged time of deposition where a thicker layer of the Co deposit can be formed.

To study the alloying behaviour during Co deposition, a carefully controlled anodic potential excursion was applied and the surface morphological change was monitored. The tip shielding effect was excluded by selecting an area on the surface that has not experienced tip scanning. As shown in figure 5(a), the thicker film is composed of aggregates of Co granules of 3∼4 nm. The total amount of the Co in the film is still limited so that the single-crystal features of the Au(111) such as terraces and steps remain clearly seen. The outer layer of the Co granules can be partially removed at potentials positive of −1.4 V. Since the potential range from −1.3 to −0.9 V is within the window in which surface restructuring occurs in ionic liquid, anodic stripping was controlled to jump over that potential region and the surface was monitored at −0.5 V and −0.1 V, respectively. Stripping of the Co film at −0.5 V leads to partial exposure of the Au surface with some isolated Co islands still remained on the rest of the surface, figure 5(b). Regardless of a few hollow defects, this situation is similar to that in figure 3(b) in the island stage of Co deposition. Complete stripping of the Co film at −0.1 V in 45 min. results in the appearance of tiny but densely arranged pits, figure 5(c), that are clearly distinguishable from the hollow defects in figure 5(b). The results indicate that surface alloying has been formed at the stage after the transition from Co clusters to Co islands. However, alloying does not seem to develop into bulk severely even after prolonged deposition.

4. Conclusions

The main finding of the present work is that Co deposition on Au(111) from $CoCl_2$ in $BMIBF_4$ is characterized by (1) preferential nucleation at the structure imperfections with formation of monoatomic-height clusters of 2~3 nm in diameter, and (2) transition of the clusters to islands of 3~4 nm after prolonged deposition. The dislocation-mediated nucleation is similar to that in UHV but in contrast with the layer-by-layer growth in aqueous solutions. Furthermore, the deposition process is thermodynamically difficult with much more negative potential for deposition than that in aqueous solutions and even that from $Co(BF_4)_2$ in the same ionic liquid. These differences are mainly the results of the different existing forms of Co(II) in the solutions depending on both the solvents and the counter ions (anion). It is worthwhile emphasizing that electrodeposition in ionic liquid is not only advantageous in preparing practically more important metals and semiconductors with *in situ* STM characterization, but also provides new information valuable for elucidating the role of the solvent in electrodeposition.

Acknowledgement

The authors gratefully acknowledge financial support by the NSF of China (nos. 20021002, 20273056), Ministry of Science and Technology of China (no. 2001CB610506), Education Committee of China and Key Scientific Project of Fujian Province, China (no. 2005HZ01-3).

References

[1] W. de Heer, Confinement and size effects in free metal clusters. In *Metal Clusters at Surfaces*, K.H. Meiwes-Broer (Ed.), pp. 1–36, Springer, Berlin (2000).
[2] F.J. Himpsel, J.E. Ortega, G.J. Mankey, R.F. Willis. Magnetic nanostructures. *Adv. Phys.*, **47**, 511 (1998).
[3] B. Voigtländer, G. Meyer, N.M. Amer. Epitaxial growth of thin magnetic cobalt films on Au(111) studied by scanning tunneling microscope. *Phys. Rev. B*, **44**, 10354 (1991).
[4] J.A. Meyer, L.D. Baikie, E. Kopatzki, F.J. Behm. Preferential island nucleation at the elbows of the Au(111) herringbone reconstruction through place exchange. *Surf. Sci.*, **365**, L647 (1996).
[5] R.Q. Hwang, M.C. Bartelt. Scanning tunneling microscopy studies of metal on metal epitaxy. *Chem. Rev.*, **97**, 1063 (1997).
[6] O. Fruchart, M. Klaua, J. Barthel, J. Kirschner. Self-organized growth of nanosized vertical magnetic Co pillars on Au(111). *Phys. Rev. Lett.*, **83**, 2769 (1999).
[7] I. Chado, S. Padovani, F. Scheurer, J.P. Bucher. Controlled nucleation of Co clusters on Au(111): towards spin engineering. *Appl. Surf. Sci.*, **164**, 42 (2000).
[8] S. Rohart, G. Baudot, V. Repain, Y. Girard, S. Rousset, H. Bulou, C. Goyhenex, L. Proville. Atomistic mechanisms for the ordered growth of Co nanodots on Au(7 8 8): a comparison between VT-STM experiments and multi-scaled calculations. *Surf. Sci.*, **559**, 47 (2004).
[9] D. Hofmann, W. Schindler, J. Kirschner. Electrodeposition of nanoscale magnetic structures. *Appl. Phys. Lett.*, **73**, 3279 (1998).
[10] L. Cagnon, A. Gundel, T. Devolder, A. Morrone, C. Chappert, J.E. Schmidt, P. Allongue. Anion effect in Co/Au111) electrodeposition: structure and magnetic behavior. *Appl. Surf. Sci.*, **164**, 22 (2000).
[11] M. Kleinert, H.-F. Waibel, G.E. Engelmann, H. Martin, D.M. Kolb. Co deposition on Au(111) and Au(100) electrodes: an *in situ* STM study. *Electrochim. Acta*, **46**, 3129 (2001).
[12] T. Cohen-Hyams, W.D. Kaplan, J. Yahalom. Structure of electrodeposited cobalt. *Electrochem. Solid-State Lett.*, **5**, C75 (2002).

[13] L.H. Mendoza-Huizar, J. Robles, M. Palomar-Pardavé. Nucleation and growth of cobalt onto different substrates. Part II. The upd-opd transition onto a gold electrode. *J. Electroanal. Chem.*, **545**, 39 (2003).
[14] P. Allongue, L. Cagnon, C. Gomes, A. Gündel, V. Costa. Electrodeposition of Co and Ni/Au(111) ultrathin layers. Part I: nucleation and growth mechanisms from *in situ* STM. *Surf. Sci.*, **557**, 41 (2004).
[15] J.S. Wilkes, M.J. Zaworotko. Air and water stable 1-ethyl-3-methylimidazolium based ionic liquids. *Chem. Commun.*, 965 (1992).
[16] T. Nishida, Y. Tashiro, M. Yamamoto. Physical and electrochemical properties of 1-alkyl-3-methylimidazolium tetrafluoroborate for electrolyte. *J. Fluorine Chem.*, **120**, 135 (2003).
[17] M.C. Buzzeo, R.G. Evans, R.G. Compton. Non-haloaluminate room-temperature ionic liquids in electrochemistry – A review. *Chem. Phys. Chem.*, **5**, 1106 (2004).
[18] F. Endres, S.Z.E. Abedinw. Air and water stable ionic liquids in physical chemistry. *Phys. Chem. Chem. Phys.*, **8**, 2101 (2006).
[19] F. Endres. Ionic liquids: Solvents for the electrodeposition of metals and semiconductors. *Chem. Phys. Chem.*, **3**, 144 (2002).
[20] F. Endres. Ionic liquids: Promising solvents for electrochemistry. *Z. Phys. Chem.*, **218**, 255 (2004).
[21] F. Endres, M. Bukowski, R. Hempelmann, H. Natter. Electrodeposition of nanocrystalline metals and alloys from ionic liquids. *Angew. Chem. Int. Ed.*, **42**, 3428 (2003).
[22] W. Freyland, C.A. Zell, S. Zein El Abedin, F. Endres. Nanoscale electrodeposition of metals and semiconductors from ionic liquids. *Electrochim. Acta*, **48**, 3053 (2003).
[23] C.A. Zell, W. Freyland. *In situ* STM and STS study of Co and Co–Al alloy electrodeposition from an ionic liquid. *Langmuir*, **19**, 7445 (2003).
[24] J.A. Mitchell, W.R. Pitner, C.L. Hussey, G.R. Stafford. Electrodeposition of cobalt and cobalt–aluminum alloys from a room temperature chloroaluminate molten salt. *J. Electrochem. Soc.*, **143**, 3448 (1996).
[25] P. He, H.T. Liu, Z.Y. Li, J.H. Li. Electrodeposition of platinum in room-temperature ionic liquids and electrocatalytic effect on electro-oxidation of methanol. *J. Electrochem. Soc.*, **152**, E146 (2005).
[26] P. He, H.T. Liu, Z.Y. Li, Y. Liu, X.D. Xu, J.H. Li. Electrochemical deposition of silver in room-temperature ionic liquids and its surface-enhanced Raman scattering effect. *Langmuir*, **20**, 10260 (2004).
[27] P.-Y. Chen, I.W. Sun. Electrodeposition of cobalt and zinc_cobalt alloys from a lewis acidic zinc chloride-1-ethyl-3-methylimidazolium chloride molten salt. *Electrochim. Acta*, **45**, 441 (1999).
[28] L.G. Lin, Y. Wang, J.W. Yan, Y.Z. Yuan, J. Xiang, B.W. Mao. An *in situ* STM study on the long-range surface restructuring of Au(111) in a non-chloroaluminumated ionic liquid. *Electrochem. Commun.*, **5**, 995 (2003).
[29] A.C. Tseung, C.Q. Cui, S.P. Jiang. Electrodeposition of cobalt from aqueous chloride solutions. *J. Electrochem. Soc.*, **137**, 3418 (1990).
[30] U. Schroder, J.D. Wadhawan, R.G. Compton, F. Marken, P.A.Z. Suarez, C.S. Consorti, R.F. de Souza, J. Dupont. Water-induced accelerated ion diffusion: voltammetric studies in 1-methyl-3-[2,6-(S)-dimethylaten-2-yl]imidazolium tetrafluoroborate, 1-butyl-3-methylimidazolium tetrafluoroborate and hexafluorophosphate ionic liquids. *New J. Chem.*, **24**, 1009 (2000).